Acute Pulmonary Toxicity Caused by Single Intratracheal Instillation of Various Doses of Colloidal Silver Nanoparticles in Mice: Pathological Changes, Particle Bioaccumulation and Metallothionien Protein Expression

Theerayuth Kaewamatawong [1*] Wijit Banlunara[1] Pattwat Maneewattanapinyo[2]

Chuchaat Thammacharoen[2] Sanong Ekgasit[2]

Abstract

To study acute lung toxicity of various doses of colloidal silver nanoparticles (Ag-NPs), mice were intratracheally instilled with 0, 10, 100, 1000 or 10,000 ppm of Ag-NPs. Histopathology, autometallography (AMG) and immunohistochemistry were determined at 1, 3, 7 and 15 days post-exposure.Instillation of 100, 1,000 and 10,000 ppm Ag-NPs produced moderate to severe necrotizing bronchitis and alveolitiswith hypertrophy and hyperplasia of alveolar epithelial cells. The severity of the pulmonary inflammation and damage increased in a dose-dependent manner. Concomitant lamininimmunohistochemical findings generally correlated with pulmonary lesions. Interleukin 1- beta (IL-1β) and tumor necrotic factor-alpha (TNF-α) positive immunostaining were found in the inflammatory lesions in lungs of treated animals. Superoxide dismutase (SOD) and metallothionine (MT) expression occurred in particle laden AMs and lung epithelial cells, which correlated with inflammatory sites and particle aggregated areas. AMG gains were found inparticle laden AMs, alveolar epithelial cells and macrophages in hilarlymph nodes. These findings suggest that instillation of AgNPs causes acute lung inflammation and tissue damage in a concentration-dependent manner. IL-1β and TNF-α may involve in the pathogenesis of the acute lung toxicity. Oxidative stress may underlie the lung tissue injury. Moreover, the expression of MT in tissues responded to AgNPs accumulation.

บทคัดย่อ

ความเป็นพิษระยะเฉียบพลันของระบบทางเดินหายใจของหนูเมาส์ที่สัมผัสอนุภาคนาโนแร่เงิน ระดับความเข้มข้นต่างๆ : การศึกษาด้านพยาธิวิทยา การสะสมของอนุภาค และการตอบสนอง ของโปรตีนเมทัลโลไธโอนีน

ธีระยุทธ แก้วอมตวงศ์ [1] วิจิตร บรรลุนารา [1] ภัททวัฒน์ มณีวัฒนภิญโญ [2] ชูชาติ ธรรมเจริญ [2] สนอง เอกสิทธิ์ [2]*

เพื่อศึกษาความเป็นพิษระยะเฉียบพลันของอนุภาคนาโนแร่เงิน ในระดับความเข้มข้นต่างๆ ต่อระบบทางเดินหายใจของหนูเมาส์ ทำการสอดท่อผ่านทางหลอดลมของหนูแล้วหยดอนุภาคนาโนแร่เงินขนาด 0 10 100 1000 หรือ 10,000 พีพีเอ็ม จากนั้นในวันที่ 1 3 7 และ 15 ทำการการุณยฆาตและเก็บตัวอย่างชิ้นเนื้อเพื่อศึกษาทางพยาธิวิทยา ย้อมออโตเมทัลโลกราฟฟี และย้อมอิมมูโนฮีสโตเคมี จากการศึกษา ทางพยาธิวิทยา พบว่าการได้รับอนุภาคนาโนแร่เงินในระดับ 100 1,000 และ 10,000 พีพีเอ็ม ทำให้หลอดลมและถุงลมฝอยของปอดอักเสบ ปานกลางถึงรุนแรงแบบมีเนื้อตาย และพบการเพิ่มจำนวนและขยายขนาดของเซลล์เยื่อบุถุงลมฝอย ซึ่งความรุนแรงของรอยโรคแปรผันตาม ระดับความเข้มข้นของสารที่ได้รับ จากการย้อมด้วยอิมมูโนฮีสโตเคมีของลา-มีนินพบความเสียหายของเยื่อรองรับฐานของปอดซึ่งสัมพันธ์กับ รอยโรคปอดที่เกิดขึ้น พบผลบวกในการย้อมอิมมูโนฮีสโตเคมีของอินเตอร์ลิวคิน-1 เบต้า และ tumor necrotic factor-alpha ในบริเวณที่ มีรอยโรคของปอด จากการศึกษาการปรากฏของซุปเปอร์ออกไซด์ดิสมิวเตสและการแสดงออกของโปรตีนเมทัลโลไธโอนีนพบการติดสีบริเวณ เซลล์แมคโครฟาจที่เก็บกินอนุภาคและเซลล์เยื่อบุของปอดในบริเวณที่พบรอยโรคของปอดและบริเวณที่มีการสะสมของอนุภาค จากการย้อม ออโตเมทัลโลกราฟฟีเพื่อศึกษาการสะสมของอนุภาคนาโนแร่เงินพบผลบวกในเซลล์แมคโครฟาจและเซลล์เยื่อบุของปอดที่เก็บกินอนุภาค รวมทั้งในเซลล์แมคโครฟาจในต่อมน้ำเหลืองขั้วปอด จากผลการทดลองทั้งหมดสรุปได้ว่า การสัมผัสอนุภาคนาโนแร่เงินสามารถทำให้ปอด อักเสบและเสียหายได้ โดยความรุนแรงขึ้นกับระดับความเข้มข้นที่สัมผัส จากการศึกษาพยาธิกำเนิดพบว่า อินเตอร์ลิวคิน-1 เบต้า tumor necrotic factor-alpha และอนุมูลอิสระมีความเกี่ยวข้องในขบวนการอักเสบและความเสียหายที่เกิดขึ้น และพบว่าการปรากฏของโปรตีน เมทัลโลไธโอนีนมีความเกี่ยวข้องกับการสะสมของอนุภาคนาโนแร่เงิน

คำสำคัญ: ระยะเฉียบพลัน อนุภาคนาโนแร่เงิน การหยดสารผ่านหลอดลม ความเป็นพิษต่อปอดหนูเมาส์

[1] *ภาควิชาพยาธิวิทยา คณะสัตวแพทยศาสตร์ จุฬาลงกรณ์มหาวิทยาลัย ปทุมวัน กรุงเทพฯ 10330*
[2] *หน่วยปฏิบัติการวิจัยอุปกรณ์รับรู้ภาควิชาเคมีคณะวิทยาศาสตร์จุฬาลงกรณ์มหาวิทยาลัย ปทุมวัน กรุงเทพฯ 10330*
 *ผู้รับผิดชอบบทความ E-mail: *theerayuth71@hotmail.com*

Introduction

Silver nanoparticles (Ag-NPs) have been known to have inhibitory and bactericidal effects as well as to be effective in retarding growth of mold, harmful spores and germs. Ag-NPs are used and applied in a wide range of applications, especially in health applications and textile industry (Chen and Schluesener, 2008). *In vitro* studies reveal cytotoxic effects of Ag-NPs including reducing cell viability, damaging cell membrane and interrupting the biological effects of theepithelial and mesenchymal cells. These toxic effects were related to generation of reactive oxygen species (ROS) that affects mitochondrial function (Medina et al., 2007).There are few studies of *in vivo* pulmonary toxicity of Ag-NPs. These reports demonstrated the distribution of Ag-NPs in the lung and systemic organs including liver, kidney, spleen, brain, and heart with rapid clearance from the organs then enter systemic pathway (Takenaka et al., 2001). For pathological effects, there were no significant health impacts of acute inhalation exposure to Ag-NPs. However, subacute exposure to Ag-NPs showed slight pulmonary inflammation and cytotoxicity (Stebounova et al., 2011).The underlying causes and pathogenesis of Ag-NPs toxicity are still largely unclear.

IL-1β and TNF-α, major proinflammatory cytokines involved in acute inflammation and tissue injury, often act synergistically in complex regulation on signaling molecules or protein expression in animal or human diseases (Kolb et al., 2001). Several studies have described important roles of IL-1β and TNF-α in lung injury caused by exposure to ambient

particles. Alveolar macrophages that exposed particulate particles release TNF-α and IL-1β, which induce expression of proinflammatory mediators such as nuclear factor kappa-l (NF-κB) and activator protein 1 (AP-1). Both proinflammatory mediators activate binding of transcription factors to the enhancers of the mediator genes that is important to inflammatory process (Ishii et al., 2004; Mukhopadhyay et al., 2006).

Nanoparticles have been reported to cause oxidative stress as a result of the generation of ROS in a number of *in vivo* and *in vitro* studies (Dick et al., 2003; Donaldson and Stone, 2003; Kaewamatawong et al., 2006). *In vivo* study of nanosilver also revealed the cytotoxicity of particles that were related to the generation of ROS (Choi et al., 2010; Miura and Shinohara, 2009).

Metallothionein (MT), a low molecular weight and cystein-rich protein, can regulate essential metals such as Zn and plays an important role in detoxification of non-essential metal ions such as Ag, Cd, Pb and Hg (Nordberg and Nordberg, 2009). Several laboratory and field studies noted that metallothionein (MT) played an important role in heavy metal homeostasis and detoxification in animals. Expression of MT in tissues responded heavy metal exposure has been reported in various kinds of organisms and animals (Alvarado et al., 2006; Kaewamatawong et al., 2012). The protective role of MT to silver nanomaterials is still unknown. There is no report of MT expression in *in vivo* study caused by exposure to Ag-NPs.

To demonstrate pulmonary basement membrane damage caused by exposure to AgNPs, expression of laminin was used as representative by immunostaining. Laminin is an intrinsic component of all basement membranes and plays a central role in the formation, architecture, and stability of basement membranes as well as the control of cellular interactions. It can be used as a marker of pulmonary basement membrane injury because it is present along the alveoli throughout the lung (Aumailley and Smyte, 1998).

To study the deposition of our Ag-NPs, autometallography (AMG) was performed. Several toxicity studies of heavy metal used AMG technique to detect small amount of the metal in the cells of various kinds of animals (Danscherand Stoltenberg, 2006). In this study, we tried to use this technique to detect *in situ* AgNPs in lung and lymph node parenchyma.

The purpose of this study was to elucidate the potential toxic effects associated with single intratracheal instillation of Ag-NPs using mouse model for pulmonary histopathological changes during acute stage. The pathogenesis of pulmonary toxicity of Ag-NPs relating to the proinflammatory cytokines and reactive oxygen species, and the protective role of metallothionein were elucidated using immunohistochemistry. Moreover, the distribution and accumulation of Ag-NPs were investigated by histochemical autometallography.

Materials and Methods

Experimental animal: Seven to eight week-old male ICR mice were purchased from National Laboratory Animal Centre, Mahidol University, Thailand. The animals were kept in an animal facility that of which the light/dark cycle was control under 12:12 hr, temperature of 25 ± 1^0C and relative humidity of $55\pm10\%$. The mice were fed mouse chow and given filtered tap water ad libitum throughout the experiment. All protocols of animal experiments were approved by the ethics committee of Chulalongkorn University Animal Care and Use Committee (CU-ACUC; Approval No. 12310080).

Particles: Colloidal silver nanoparticles were acquired from Sensor Research Unit, Department of Chemistry, Faculty of Science, Chulalongkorn University, Thailand. Preparation protocol of AgNPs was described in our previous study (Maneewattanapinyo et al., 2011). Briefly, a 0.094 M aqueous solution of silver nitrate ($AgNO_3$; Merck) was added dropwise to an aqueous solution of 0.07 M sodium borohydride ($NaBH_4$; Merck) under a vigorous stir. Soluble starch (Merck) was used as stabilizer and solvent in the mixing processes. Purification of the AgNPs was precipitated using centrifugation. Percentage of purity of the AgNPs measured by macro- and microelectrode was 99.96%. Ag ions concentraion in Ag-NPs was less than 0.04%. The Ag-NPs had a spherical configuration with a relatively uniform size distribution approximately 10-20 nm on average. To obtain various concentrations of AgNPs, the Ag-NPs were suspended in distilled water prior to use.

Experimental design: Sixty male ICR mice were singly intratracheally instilled with 50 µl aqueous suspensions of 10, 100, 1000 or 10,000 ppm of Ag-NPs suspensions. The control group of mice was instilled with 50 µl of distilled water. One, 3, 7 and 15 days after instillation, the animals in each group were sacrificed. Lungs and hilar lymph nodes were collected in 10% buffered neutral formalin forroutine histopathological evaluations and immunohistochemistry.

Immunohistochemistry protocol: Tissue samples from lungs and lymph nodes of the control and treated animals were immunostained to detect pulmonary basement membranes (laminin), proinflammatory cytokines (TNF-α, IL-1β), antioxidant enzymes (Cu/Zn SOD), and MT. After deparaffinization, the sections were treated with proteinase K for 30 min at 39^0C (for detection of laminin) or with citrate buffer solution (pH = 5.4-6.0; for detection of TNF-α, IL-1β, Cu/Zn SOD and MT) for 20 min at 121^0C by autoclave and microwave heat at 700 W for 5 min in the process of antigen retrieval. The sections were incubated with 3% H_2O_2 in methanol to quench endogenous peroxidase for 30 min at room temperature.The slides were then blocked with 10% normal goat serum (laminin, TNF-α and Cu/Zn SOD) for 5 min in microwave oven at 250 W or 1% bovine serum albumin (IL-1β and MT) for 30 min at 37^0C. Thereafter, the sample and positive control sections were incubated overnight at 4^0C with primary antibodies (monoclonal rabbit anti- laminin Ab, 1 : 200

dilution; polyclonal rabbit anti TNF-α Ab, Monosan, Uden, the Netherlands, 1 : 15 dilution; polyclonal rabbit anti-IL-1β Ab, Santa Cruz Biotechnology, Santa Cruz, CA, 1 :00 dilution; polyclonal rabbit anti-Cu-Zn SOD Ab, Stressgen Bioreagents, Victoria, Canada, 1 : 200 dilution; and monoclonal mouse anti-MT Ab, Dako®, Glostrup, 1 : 50 dilution). For the negative control sections, they were incubated with phosphate buffered saline. The biotinylated anti-mouse IgG antibody and EnVision polymer (Dako^REALTM EnVision™ detection system, Dako®, Denmark) was applied to the sections as a secondary antibody. Brown staining with the substrate 3,3'-diaminobenzidine tetrahydrochloride (DAB) was determined as positive result and the sections were counterstained with Mayer's hematoxylin for 30 sec.

Autometallography staining: Lung and hilar lymph nodes from the control and treated mice were investigated for the presence of Ag-NPs distribution and accumulation. After deparaffinization, the sections were incubated with 1% potassium cyanide for 2 hours to eliminate other metal residues and then rinsed well with tap water and distilled water (DW). For silver amplification, physical developer (50% Arabic gum, 50% citrate buffer, 5.6% hydroquinone and 17% AgNO$_3$) was applied to the sections 1 hr in automatic shaker at 26^{0}C. Thereafter, the sections were reacted with 10% sodium thiosulfate and Farmer's solution (20% sodium thiosulfate and 7.5% potassium ferric cyanide) to eliminate silver residues. The sections were rinsed in tap water and counterstained with Mayer's hematoxylin. Positive reactions resulted in yellow-brown to black silver grains.

Results

Clinical and gross findings: In the control group and the 10 and 100 ppm of Ag-NPs treated groups, there were no exposure related clinical signs in any time. Forty percent of the mice in the 1,000 and 10,000 ppm treated groups showed a sign of dyspnea shortly after instillation. However, this sign recovered 6 hours post-exposure. Grossly, the instillation of 10 and 100 ppm Ag-NPs caused mild congestion and edema in the lungs. In both 1,000 and 10,000 ppm Ag-NPs treated animals, tiny pin-head sized to patchy black brown foci scattered in the lung lobes throughout the experiment (Fig 1). The degree of lesions described above in 10,000 ppm treated group was more severe than 1,000 ppm treated group.

Histopathology: One day after the instillation, accumulation of free aggregated particles was found in the alveoli and bronchiolar lumens of all treated groups. Some of the aggregated particles were present within alveolar macrophages, and occasionally present within alveolar epithelial cells with increasing number of cells in alveolar wall (Fig 2A). The animal instilled with 1,000 and 10,000 ppm Ag-NPs had severe accumulation of neutrophils, active alveolar macrophages (AMs) and Ag-NPs laden AMs in aggregated areas (Fig 2B). Three days after the instillation, the lungs from 1,000 and 10,000 ppm Ag-NPs treated groups revealed severe multifocal alveolitis characterized by accumulation of numerous active AMs, particle-laden AMs, and neutrophils with some necrotic cells. Proliferation of alveolar type II epithelial cells were also noted in the affected areas (Fig 2C). the 100 ppm Ag-NPs treated group showed similar lesions but less severe pulmonary lesions.
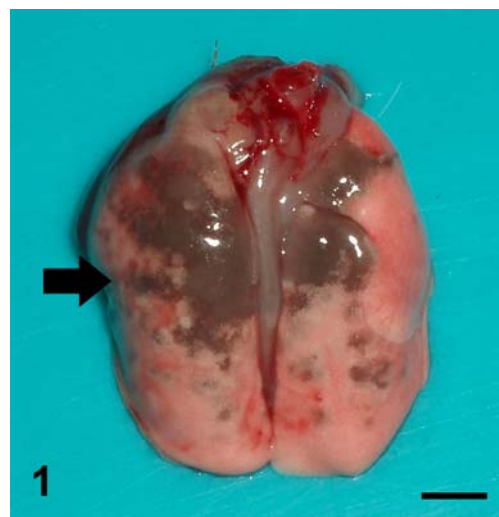

Figure 1 Lung from 10,000 ppm Ag-NPs treated animals at 1 day post-exposure shows patchy black brown foci (Bold arrow) scattered in lung lobes. (Bar = 1 cm)
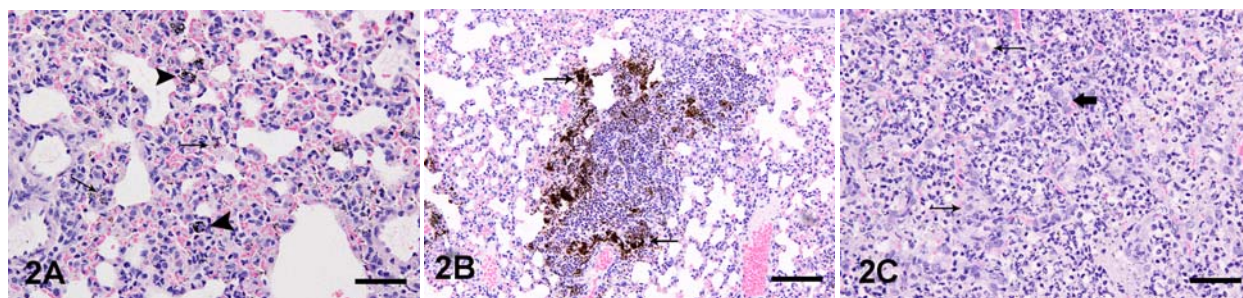

Figure 2 Lung sections from various doses of Ag-NPs treated groups at various time points, H&E stain. (A) Distributions of DEPs in AMs (arrowheads) and alveolar epithelium (arrowheads); 1.000 ppm treated group at 1 day post-exposure, Bar = 600 μm. (B) Influx of neutrophils and accumulation of particle laden AMs in Ag-NPs (arrowheads) aggregated areas; 10,000 ppm treated group at 1 day post-exposure, Bar = 250 μm. (C) Focal necrotizing alveolitis with hyperplasia of alveolar type II epithelial cells; 10,000 ppm treated group at 3 day post-exposure, Bar = 700 μm

Moderate congestion with particle laden AMs and alveolar epithelium were seen in the lungs of the 10 ppm Ag-NPs treated groups. Seven days after the instillation of Ag-NPs, severe loss of lung architecture, cellular necrosis, neutrophil infiltration, and alveolar type II proliferation were noted in the lungs of the 1,000 and 10,000 ppm treated groups. Aggregated particles and particle laden AMs were also seen in some areas of lung parenchyma. The 100 ppm Ag-NPs treated groups induced similar histopathological patterns, but the lesions were milder and occupied a small area of the lung specimens. Mild congestion was observed in the lungs from 10 ppm Ag-NPs treated groups. The lungs of mice killed at 15 days post-exposure had similar appearances and severity of lesions to those observed at 7 days post-exposure. The lesions of adjacent lymph nodes were also elucidated. The hilar lymph nodes of treated animals at 1 and 3 days post-exposure were slightly enlarged with mild to moderate particle laden macrophages and neutrophil infiltration in subcapsular and medullary sinus. At 7 days post-exposure, multifocal necrosis of lymphoid cells and mild to moderate histiocytic infiltration were noted with mild to moderate particle laden macrophage infiltration. The lungs from the 15 day post-exposure groups showed similar but greater severe lesions than those from the 7 day post-exposure groups.

Immunohistological evaluation

Laminin: Thin lines of intense brown positive laminin stains were observed along the basement membranes of alveolar septa, bronchus, bronchioles, blood vessels and bronchial glands in the control mice (Fig 3A). Lung tissues from Ag-NPs treated mice showed extensive patchy areas of nonstain or weak positive reaction and discontinuous pattern of the alveolar basement membranes in site of the inflammatory foci (Fig 3B). The interruption and weak positive immunoreactivity were also seen in the alveoli enclosing to the Ag-NPs aggregation or particle laden AMs accumulation. The severity and distribution of the lesions were in dose dependent manner and showed no different intensity during the exposure dates.

Inflammatory cytokine: IL-1 and TNF

IL-1β: The expression of IL-1β was occasionally observed in some alveolar macrophages in the control group. However, the IL-1β expression was mainly in the cytoplasm of particle laden AMs and active AMs, and
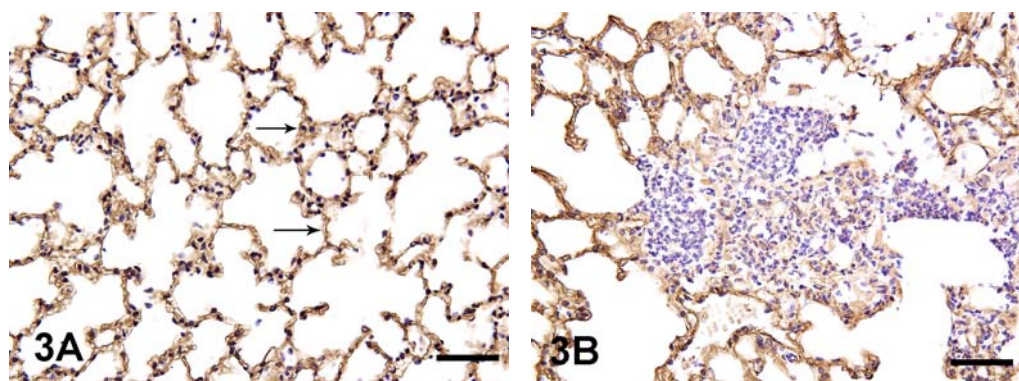
Figure 3 Laminin immunohistochemistry in lungs of control and Ag-NPs-treated mice sacrificed at 3 days post-exposure. (A) Brown thin string-like positive staining along alveolar basement membranes (arrows) in control animals, Bar = 300 μm (B) Weak and discontinuous positive patterns of alveolar basement membrane at focal alveolitis in Ag-NPs-treated mice, Bar = 600 μm.
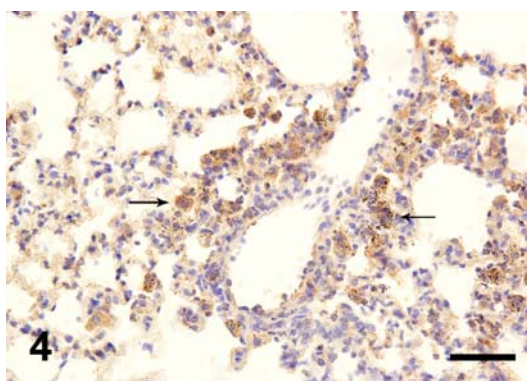
Figure 4 Intense brown positive immunostaining of IL1-β appears in a large number ofparticle laden AMs (arrows) in lungs of 10,000 ppm group killed at 7 days post-exposure, Bar = 600 μm.
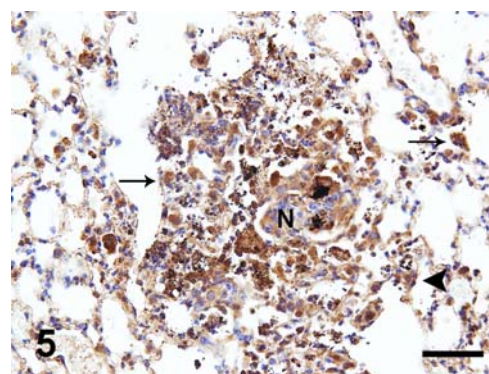
Figure 5 Prominent brown positive immunostaining of TNF-a is found mainly in particle laden AMs (arrows) and occasionally in bronchiolar epithelial cell (arrowheads) associated with inflammatory nodules (N) in lungs of 10,000 ppm group killed at 3 days post-exposure, Bar = 600 μm.

occasionally in bronchiolar epithelium of the lungs from the mice exposed to Ag-NPs at 1 to 15 days post-exposure (Fig 4).

TNF-α: In the control group, the expression of TNF-α was barely detectable in both airway epithelium and lung parenchyma. In contrast, in the Ag-NPs-treated mice at 1-15 days post-exposure, positive staining for TNF-α appeared in a large number of cells associated with pulmonary inflammation. TNF-α was expressed mainly in the cytoplasm of particle laden AMs and active AMs, and occasionally in bronchiolar epithelium that associated with inflammatory nodules and necrotic areas (Fig 5).

SOD: The expression of *SOD* was seen in small number of AMs in the control animals. After 1-15 days, SOD expression was observed chiefly in particle laden and activated AMs, and moderately in bronchiolar epithelial cells that associated with the inflammatory sites and particle aggregated areas but minimally in alveolar epithelial cells (Fig 6).

Metallothionine(MT-1 and MT-2): In the Ag-NPs-treated mice at 1 to 15 days post-exposure, positive staining for MT appeared in a large number of cells associated with aggregated nodules and areas that enclose to particle laden AMs. MT was expressed mainly in the cytoplasm of particle laden and active AMs and occasionally detectable in bronchiolar and alveolar epithelial cells (Fig 7). In contrast, the immunohistochemical staining of MT was barely detectable in the cytoplasm of airway epithelium in the control animals.

Autometallography: The deposition of Ag-NPs characterized by black positive silver grains were observed in the cytoplasm of particle laden AMs and alveolar epithelium (Fig 8). The large number of positive cells and clump of free black grains appeared in the area of inflammatory nodules. Degrees and distribution of Ag-NPs positive staining showed a trend toward increasing in a dose-dependent manner, but not different among the exposure days. On the other hand, no evidence of positive silver grains was found in the lungs from the control group.

Discussion

The purpose of this study was to determine the pathological effects of intratracheal instillation of various doses of Ag-NPs on the lungs of mice in terms of dose response during the acute stage. Possible mechanisms for the pulmonary injury involving inflammatory changes and tissue damage were discussed. In addition, the distribution of the Ag-NPs in lung tissues and the protective role of MT were also elucidated.

Subacute inhalation study of 1 ppm commercial Ag-NPs revealed no pathologic changes including alveolitis, perivasculitis, lymphoid agglomerates, epithelial damage, granulomas, giant cells or fibrosis (Stebounova et al., 2011). In our pilot study, we also found that the single instillation of 1 ppm Ag-NPs revealed no significant pathological lesions in all observation times.
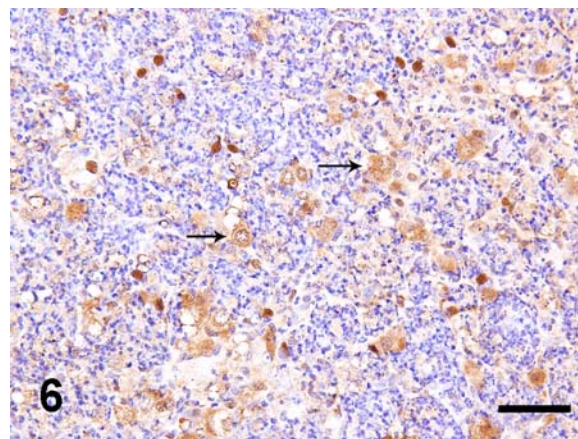

Figure 6 Intense positive labeling of SOD is expressed in cytoplasm particle laden AMs (arrows) located at inflammatory nodules in lung of 1,000 ppm group killed at 15 days post-exposure, Bar = 700 µm.
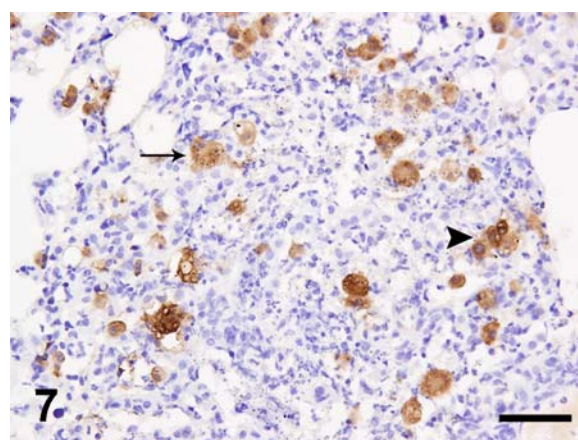

Figure 7 Immunohistochemical localization of MT in lungs of 1,000 ppm group sacrificed at 7 days post-exposure, brown positive staining was observed in particle laden AMs (arrows) and active AMs (arrowheads), Bar = 600 µm.
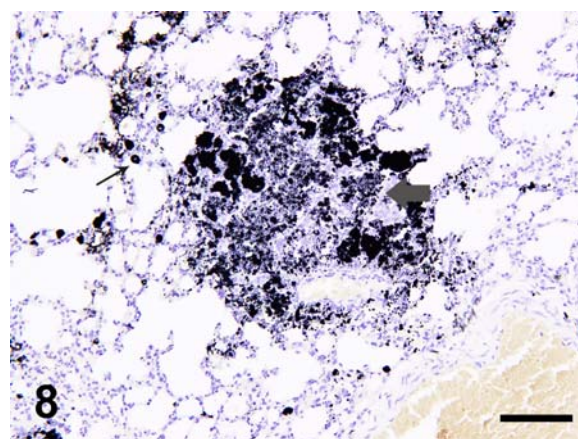

Figure 8 Black positive silver grains in lungs of 10,000 ppm group sacrificed at 1 day post-exposure were observed in cytoplasm of particle laden AMs (arrow) and clump of Ag-NPs appeared in the area of inflammatory nodules (Bold arrow), Bar = 600 µm.

The adverse effects of nanoparticles on the pulmonary basement membranes were reported in nanotoxicity murine models (Kaewamatawong et al., 2005; Shimada et al., 2006). In mice exposed to Ag-NPs in this study, we showed the direct effects of Ag-NPs on the basement membranes as evidence of weak and discontinuous positive stainings of laminins along the alveoli that refer to the aggregation of Ag-NPs. The disturbance of the equilibrium between the synthesis and degradation changes of pulmonary extracellular matrix (ECM) including laminin may result in pulmonary fibrosis (Dunsmore and Rannels, 1996). The accelerated degradation of the ECM as present in the weakened positive immunolabeling for laminin in the acute inflammatory lesions may develop into fibrosis in the chronic stages.

Many kinds of nanoparticles can induce the production of IL-1β and TNF-α that are responsible for the induction and modulation of chemokines in the lungs (Pryhuber et al., 2003). Many types of pulmonary cell, mainly alveolar macrophages and airway epithelial cells, can release these two cytokines. In the current study, IL-1β and TNF-α were shown to be present in the inflammatory lesions in both alveolar macrophages and airway epithelial cells of the treated mice's lungs, suggesting that these cytokines may be involved in the pathogenesis the acute lung toxicity induced by Ag-NPs.

To prevent oxidative harmful reaction, cells develop free-radical scavenging process by various kinds of antioxidant enzymes including superoxide dismutase (SOD), catalase and glutathione peroxidase. Superoxide dismutase (SOD) are primary antioxidant enzymes that scavenges the ROS by catalyzing the dismutation reaction of the superoxide anion to hydrogen peroxide. Several *in vitro* nanotoxicity studies have been revealed the association between the free-radical generation and SOD scavenging activity. Dey et al. (2008) demonstrated increases in manganese superoxide dismutase (MnSOD) protein levels induced by nanosized alumina in mouse skin epithelial cells. Decrease in SOD and glutathione (GSH) level that is associated with generation of peroxy radicals after Ag-NPs exposure to human fibrosarcoma (HT-1080) and human skin/carcinoma (A431) cells was reported (Arora et al., 2008). In our study, the results of the positive Cu/Zn SOD immunoreactivity mainly in particle laden and activated AMs associated with the inflammatory sites and some free particle aggregated areas indicate a pulmonary response to oxidant stress generated by Ag-NPs in either direct effect of particles themselves or indirect effect of inflammatory reaction.

In vitro cytotoxicity study of astrocytes exposure to Ag-NPs showed upregulation of MT via activation of metal regulatory transcription factor 1 (MTF-1)(Luther et al., 2012). Certain mechanisms associated with the MT responses to Ag-NPs exposure remains unclear. Silver (Ag) can directly stimulate the production of MT via the initiation of thionien in the cells (Kim et al., 2009). In another mechanism, enhancement of MT induction is associated with their antioxidant role that response to an increase in oxyradicals (Haq et al., 2003). In the present study, MT immuno-expression was detected in the macrophages or airway epithelium that were associated with Ag-NPs aggregated nodules and areas adjacent to particle laden AMs. We, therefore, suggest that MT might have a protective role to Ag-NPs at acute stage. The underlying mechanism of the induction of MT caused by exposure to Ag-NPs should be elucidated.

Several inhalation studies demonstrated the translocation of Ag-NPs by inductively coupled plasma mass spectrometry (ICPMS) analysis. The silver was detected mainly in the lungs and adjacent lymph nodes, but minimally in the olfactory bulb, liver, kidney, spleen, brain, heart and blood (Takenaka et al., 2001). In our study, we used AMG histochemical techniques to demonstrate the *in situ* deposition and distribution of Ag-NPs in the lungs and hilar lymph nodes. To our knowledge, this is the 1st report to use this kind of technique to detect the nano metal particles. The positive AMG gains were found markedly in the cytoplasm of the particle laden AMs as well as the macrophages in the adjacent lymph nodes, and occasionally in the alveolar epithelial cells. These results indicated that the major clearance mechanism of instilled Ag-NPs might be via phagocytosis by alveolar macrophages and lymphatic circulation. Moreover, the evidence of Ag-NPs entering the alveolar epithelium might be another clearance path and also a possible way to gain access to the blood circulation.

In summary, this study demonstrated the pulmonary pathological responses after intratracheal instillation of various doses of Ag-NPs in mice during the acute stage. Ag-NPs produced the severity of pulmonary lesions in the treated animals in a concentration-dependent manner. IL-1β and TNF-α were proinflammatory cytokines involved in the pathogenesis of the acute lung toxicity induced by Ag-NPs. We also found pulmonary response to oxidative stress in the Ag-NPs treated animals, which may be one of the underlying causes of the lung tissue injury. Furthermore, our current study found that Ag-NPs could induce the expression of MT that might be one of the protective mechanisms of lung against nanoparticles.

References

Alvarado AE, Quesada I, Hylland K, Marigomez L and Soto M 2006. Quantitative changes in metallothionein expression in target cell-types in the gills of turbot (*Scopthalmus maximus*) exposed to Cd, Cu, Zn and after a depuration treatment. Aqual Toxicol. 77: 64-77.

Arora S, Jain J, Rajwade JM and Paknikar KM 2008. Cellular responses induced by silver

nanoparticles: *in vitro* studies. Toxicol Lett. 179: 93-100.

Aumailley M and Smyte N 1998. The role of laminins in basement membrane function. J Anat. 193: 1-21.

Chen X and Schluesener HJ 2008. Nanosilver: A nanoproduct in medical application. Toxicol Lett. 176: 1-12.

Choi JE, Kim S, Ahn JH, Youn P, Kang JS, Park K, Yi J and Ryu DY 2010. Induction of oxidative stress and apoptosis by silver nanoparticles in the liver of adult Zebrafish. Aquat Toxicol. 100: 151-159.

Danscher G and Stoltenberg M 2006. Autometallography (AMG) silver enhancement of quantum dots resulting from (1) metabolism of toxic metals in animals and humans, (2) *in vivo, in vitro* and immersion created zinc-sulphur/zinc-selenium nanocrystals, (3) metal ions liberated from metal implants and particles. Progr Histochem Cytochem. 41: 57-139.

Dey S, Bakthavatchalu V, Tseng MT, Wu P, Florence RL, Grulke EA, Yokel RA, Dhar SK, Yang H, Chen Y and Clair DK 2008. Interactions between SIRT1 and AP-1 reveal a mechanistic insight into the growth promoting properties of alumina (Al$_2$O$_3$) nanoparticles. Carcinogenesis. 29: 1920-1929.

Dick CAJ, Brown DM, Donaldson K and Stone V 2003. The role of free radicals in the toxic and inflammatory effects of four different ultrafine particles types. Inhal Toxicol. 15: 39-52.

Donaldson K and Stone V 2003. Current hypotheses on the mechanisms of toxicity of ultrafine particles. AnnIst Super Sanita. 39: 405-410.

Dunsmore S and Rannels D 1996. Extracellular matrix biology in the lung. Am J Physiol. 270: 3-27.

Haq F, Mahoney M, Koropatnick J 2003. Signaling events for metallothionein induction. Mutat Res. 533: 211-226.

Ishii H, Fujii T, Hogg JC, Hayashi S, Mukae H, Vincent R and van Eeden SF. 2004.Contribution of IL-1β and TNF-α to the initiation of the peripheral lung response to atmospheric particulates (PM10). Am J Physiol Lung Cell Mol Physiol. 287: 176-183.

Kaewamatawong T, Kawamura N, Okajima M, Sawada M, Morita Tand Shimada A 2005. Acute pulmonary toxicity caused by exposure to colloidal silica: particle size dependent pathological changes in mice. Toxicol Path. 33: 743-749.

Kaewamatawong T, Shimada A, Okajima M, Inoue H, Morita T, Inoue K and Takano H 2006. Acute and subacute pulmonary toxicity of low dose of ultrafine colloidal silica particles in mice after intratracheal instillation. Toxicol Path. 34: 958-965.

Kaewamatawong T, Rattanapinyopituk K, Ponpornpisit A, Pirarat N, Ruangwises S and Rungsipipat A 2012. Short-term exposure of Nile Tilapia (*Oreochromis niloticus*) to mercury: Histopathological changes, mercury bioaccumulation, and protective role of

metallothioneins in different exposure routes. Toxicol Pathol. 41(3): 470-479.

Kim S, Choi JE, Choi J, Chung K, Park K, Yi J and Ryu D 2009. Oxidative stress-dependent toxicity of silver nanoparticles in human hepatoma cells. Toxicol Vitro.23: 1076-1084.

Kolb M, Margetts PJ, Anthony DC, Pitossi F and Gauldie J 2001. Transient expression of IL-1beta induces acute lung injury and chronic repair leading to pulmonary fibrosis. J Clin Invest. 107: 1529-1536.

Luther EM, Schmidt MM, Diendorf J, Epple M and Dringen R 2012.Upregulation of metallothioneins after exposure of cultured primary astrocytes to silver nanoparticles. Neurochem Res.37: 1639-1648.

Maneewattanapinyo P, Banlunara W, Thammacharoen C, Ekgasit S and Kaewamatawong T 2011. An evaluation of acute toxicity of colloidal silver nanoparticles. J Vet Med Sci. 73: 1417-1423.

Medina C, Santos-Martinez MJ, Radomski A, Corrigan OI and Radomski MW 2007.Nanoparticles: pharmacological and toxicological significance. Br J Pharmacol. 150:552-558.

Miura N and Shinohara Y 2009. Cytotoxic effect and apoptosis induction by silver nanoparticles in Hela cells. Biochem Biophys Res Commun. 390: 733-737.

Mukhopadhyay S, Hoidal JR and Mukherjee TK 2006. Role of TNF alpha in pulmonary pathophysiology. Respir Res. 7:1-9

Nordberg M and Nordberg GF 2009. Metallothioneins: Historical development and overview. Met Ions Life Sci. 5: 1-29.

Pryhuber G, Huyck H, Baggs R, Oberdorster Gand Finkelstein J 2003. Induction of chemokines by low-dose intratracheal silica is reduced in TNFR I (p55) null mice. Toxicol Sci. 72: 150–157.

Shimada A, Kawamura N, Okajima M, Kaewamatawong T, Inoue H and Morita T 2006. Translocation pathway of the intratracheally instilled ultrafine particles from the lung into the blood circulation in the mouse. ToxicolPathol. 34: 949–957.

Stebounova LV, Adamcakova-Dodd A, Kim JS, Heaweon, PH, O'Shaughnessy PT, Grassian VH and Thorne PS 2011. Nanosilver induces minimal lung toxicity or inflammation in a subacute murine inhalation model. Part Fibre Toxicol. 8: 1-12.

Takenaka S, Karg E, Roth C, Schulz H, Ziesenis A, Heinzmann U, Schramel P and Heyder J 2001. Pulmonary and systemic distribution of inhaled ultrafine silver particles in rats. Environ Health Perspect. 109: 547-551.